Automatic detection of the breast border and nipple position on digital mammograms using genetic algorithm for asymmetry approach to detection of microcalcifications

M. Karnan [a,*], K. Thangavel [b]

[a] Department of Computer Science and Engineering, Tamil Nadu College of Engineering, Coimbatore, Tamil Nadu, India
[b] Department of Computer Science, Periyar University, Salem, Tamil Nadu, India

ARTICLE INFO

ABSTRACT

The presence of microcalcifications in breast tissue is one of the most incident signs considered by radiologist for an early diagnosis of breast cancer, which is one of the most common forms of cancer among women. In this paper, the Genetic Algorithm (GA) is proposed for automatic look at commonly prone area the breast border and nipple position to discover the suspicious regions on digital mammograms based on asymmetries between left and right breast image. The basic idea of the asymmetry approach is to scan left and right images are subtracted to extract the suspicious region.

The proposed system consists of two steps: First, the mammogram images are enhanced using median filter, normalize the image, at the pectoral muscle region is excluding the border of the mammogram and comparing for both left and right images from the binary image. Further GA is applied to magnify the detected border. The figure of merit is calculated to evaluate whether the detected border is exact or not. And the nipple position is identified using GA. The some comparisons method is adopted for detection of suspected area. Second, using the border points and nipple position as the reference the mammogram images are aligned and subtracted to extract the suspicious region. The algorithms are tested on 114 abnormal digitized mammograms from Mammogram Image Analysis Society database.

1. Introduction

Breast cancer is one of the major causes for the increase in mortality among women, especially in developed countries. Breast cancer is the second most common cancer in women. The World Health Organization's International the first being agency for Research on Cancer in Lyon, France, estimates that more than 1,50,000 women worldwide die of breast cancer in year [4]. In India, breast cancer accounts for 23% of all the female cancer death followed by cervical cancer (17.5%) in India. Although the incidence is lower in India than in the developed countries, the burden of diagnosing and treating of breast cancer in India is alarming [15]. The incidence is more among urban than rural women. It is more prevalent in the higher socio-economic groups. The average incidence rate varies from 22 to 28 per 1,00,000 women per year in urban settings to 6 per 1,00,000 women per year in rural India. The WHO survey suggests that by 2020 there will be 10 million new cancer cases every year in the developing world, of which 6 million people will die. In India alone it is estimated that 1.5 million new cancer cases will occur yearly at the start of this century.

---

* Corresponding author. Tel.: +90 4545244385; fax: +90 4545244385.
  E-mail address: karnanme@yahoo.com (M. Karnan).
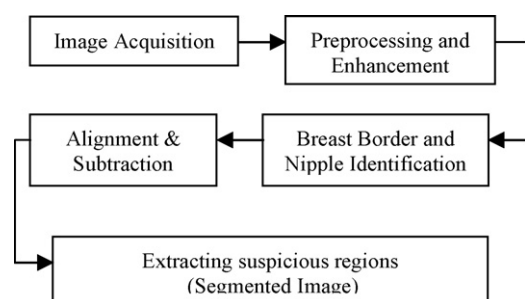
Fig. 1 – Block diagram for asymmetry approach.

Mammography has been shown to be the most effective and reliable method for early cancer detection [15]. Two different techniques are used in the interpretation of mammograms. The first technique consists of a systematic search of each mammogram for visual patterns symptomatic of tumors. The second technique, the asymmetry approach, consists of a systematic comparison of corresponding regions in the left and right breast. Significant structural asymmetries between the two regions can indicate the possible presence of a tumor [10]. Thangavel et al. [16] represented a study on methods of various stages on automatic detection of microcalcification in digital mammograms. According to that study it is stated that the GA has not been implemented in the field of mammograms image analysis. So this paper proposed to implement GA method to extract the suspicious region based on asymmetry approach.

The strategy of the asymmetry detection system can be described as follows: Given a pair of identical-view mammograms of the left and right breast, detecting all structural asymmetries between corresponding positions in the left and right breast. Significant asymmetries are taken for evidence in exploring possibilities of the cancer prevalence of a tumor. Fig. 1 shows the block diagram for asymmetry approach.

This paper, the asymmetry method is performed in two steps: First, the mammogram images are enhanced using median filter and normalized to avoid the difference between the brightness caused due to the recording procedure. Then pectoral region image is removed from the breast region image. The border of the mammogram images is detected using genetic algorithm to identify the nipple position of the mammograms. Second, the border points and nipple positions are alignment wise considered in the mammogram images. The left and right mammogram images are subtracted to find out the pronouncing structural asymmetries.

The rest of the paper is organized as follows: Section 2 presents preprocessing and enhancement techniques. Section 3 presents the border detection and the nipple identification using genetic algorithm and describes the bilateral subtraction technique. Section 4 presents the experiments and results. Section 5 describes the summary and conclusion.

2. Preprocessing and enhancement

Preprocessing and enhancement techniques are used to improve the detection of the suspicious regions in mam-

mograms. This section presents the gradient-based image enhancement method for mammography images which is based on the first derivative and the local statistics. The enhancement method consists of four processing steps; first, the removal of film artifacts such as labels and X-ray marks are removed from the mammogram. Second, the removal of high frequency components using median filtering technique [11]; third, the mammogram images are normalized to avoid the difference in brightness and contrast between the mammograms caused by the recording procedure. Fourth, the pectoral muscle region image is removed from the breast region to increase the reliability of the segmentation of microcalcifications [5,6]. The performance of the proposed method is also evaluated by means of signal-to noise-ratio (SNR) [17].

3. Breast border and nipple position identification

Segmentation of the breast region and non-breast region is a necessary prerequisite for further bilateral subtraction. The breast border can be obtained by segmenting the breast region in the image. Some authors have developed methods to identify the breast region on the basis of a global histogram analysis. However, a method based on global thresholding is critically dependent on the selection of the threshold values. Clarke et al. have developed a segmentation algorithm based on wavelet transformation [3]. Bick et al. developed a method for the analysis of the local gray value range to classify each pixel in the image [1]. Wirth and Stapinski have explored the application of active contours to the problem of extracting the breast region in mammograms [18]. Mendez et al. developed an automatic technique to detect the breast border and the nipple positions [11]. Chandrasekhar and Attikiouzel developed a method based on morphological operations for detecting the breast border [2].

The nipple may appear either in profile or not in profile. The nipple is located on the mammogram close to where the rate of change among gray levels is larger than the rest of the breast. Mendez et al. developed a gradient method: the maximum height of the breast border is taken as the position of the nipple [11]. In this paper the genetic algorithm is used to detect the breast border and identifying the nipple position. The border points and nipple position as the reference the images aligned and subtraction of the left and right breast image is performed bilateral subtraction.

3.1. Breast border detection using GA

A histogram-based thresholding technique is used to generate a binary image to separate the breast and the non-breast region. The local optimum in the histogram is selected as the threshold value. The intensity values smaller than this threshold are changed to black (zero) and the intensity values greater than the threshold are changed to white (one) in order to perform the morphological operation to remove the four-connected and eight-connected pixels in the binary image. Once the connected components are removed, the
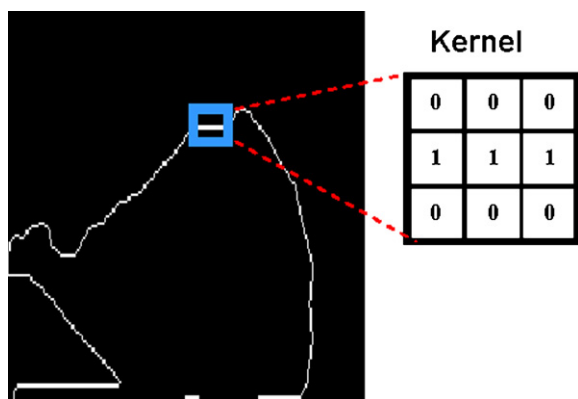
Fig. 2 – Kernel extracted from border.

Fig. 3 – Two-dimensional crossover operation.

binary image contains only the breast border. The spatial coordinates of the border points are mapped with the original gray scale mammogram image. Further, using the GA enhances to vividness the border.

GA consists of three operators such as reproduction, crossover and mutation. These operators are applied to successive string populations to create new string populations. Reproduction is a process that selects the members from the population for crossover. In crossover, random numbers of bits are exchanged between pairs of strings from the reproduced population. Mutation is the occasional random alteration with small probability of the value of the string position, which means changing bit position from one to zero and vice versa. The process of generating a new population is repeated for predetermined number of iterations [7,12].

Border detectors detect the edges in the binary images, where each pixel takes on either the intensity value zero for a non-border pixel or one for a border pixel. Each pixel in the binary map corresponds to an underlying pixel in the original image. In this proposed system, kernel is extracted from the border points as a neighborhood array of pixels of the size of 3×3 window of binary image. Fig. 2 shows the kernel extracted from border points.

The binary kernels are considered as population strings for GA. The corresponding kernels are extracted from gray level mammogram image using spatial coordinate points and the sum of intensity values is considered as the fitness value. After identifying the initial population and the fitness value, the genetic operators can be applied to generate the new population.

Reproduction operator produces a new string for crossover. Reproduction is implemented as linear search through roulette wheel with slots weighted in proportion to kernel fitness values. In this function, a random number multiplies the sum of the population fitness called as the stopping point. The partial sum of the fitness value is accumulated in a real variable until it is greater than or equal to the stopping point. The location where the iteration stops is noted and the corresponding kernel is selected for crossover. The newly reproduced kernels are crossed over by exchanging the values in the window with the size of 2×2. Figs. 3 and 4 show the 2D

crossover operation and 2D mutation operation. The kernels A and B are from the population and child A and child B is the kernels after crossing over.

Next, the mutation operator, flipping bits at random carries it out, with some small probability values. When mutation occurs on a bit string representation, a random bit is either flipped or flopped, i.e., its value is changed from zero to one or vice versa. In mutation, if the kernel that matches any one of the 14 configurations in Fig. 4 is found, the corresponding transformation is performed; otherwise no change will be made [7].

After mutation, the kernels are considered a new population. This procedure is performed until the size of the new population is equal to the initial population. Then the old population is assigned to the new population value and the same procedure is performed again to generate the next population. Finally, the kernels in the latest population are the enhanced border points. In the binary image, the spatial coordinates of the border points are mapped with the original mammogram image. Fig. 5 shows the flow diagram for breast border detection using GA. Fig. 6 shows the output result for breast border detection using GA. Fig. 7 shows the algorithm of detection of breast border using GA.
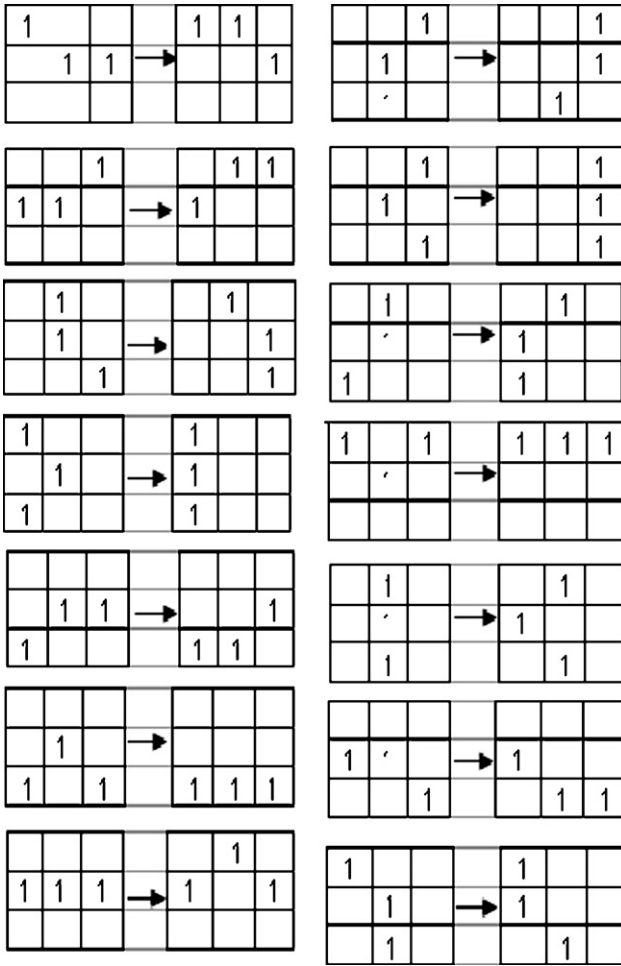
Fig. 4 – Two-dimensional mutation operation.

Fig. 5 – Breast border detection using GA.

3.2. Performance evaluation

The performance of the detected border using genetic algorithm is tested with Pratt's figure of merit [13], to compare the results of different edge detectors quantitatively. It measures the deviation of the output edge from a known ideal edge using the following formulae:

$$P = (1/\max(I_A, I_i)) \sum_i (1/(1 + \alpha d^2(i))) \quad i = 1, \dots, I_A$$

where, I_A is the number of edge points detected, I_i the number of edge points in the ideal edge image, α a scaling factor ($\alpha = 0.01$) and $d(i)$ is the distance of the detected edge pixel
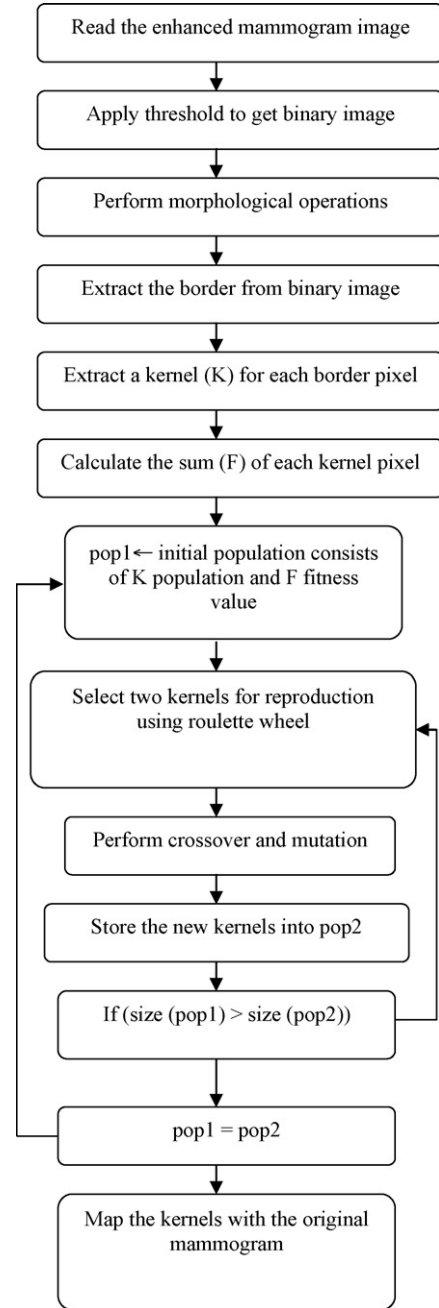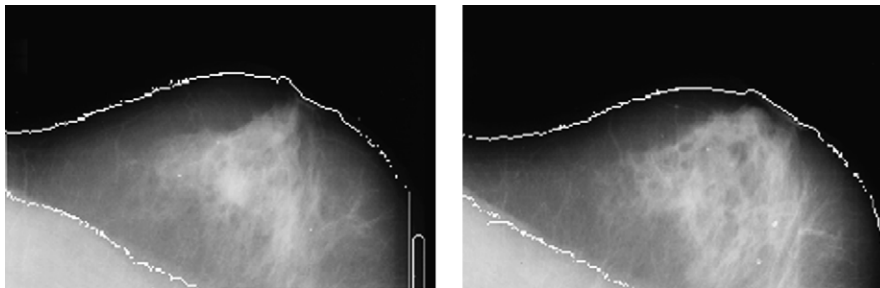

Fig. 6 – output result for border detection using genetic algorithm.

from the nearest ideal edge position. The ideal edge image is generated using logarithmic transformation.

Pratt's figure of merit is a rough indicator of edge quality. A higher value of the Pratt figure of merit gives a better edge image. Gudmundsson et al. obtained the Pratt figure of merit value 0.83 using simulated annealing (SA) [8] and Mendez et al. achieved an only 0.89 with gradient-based tracking algorithm [11]. The GA approach produces 0.93, which shows that the GA performs better than other edge detectors.

3.3. Identification of the nipple position

The intensity values of the border pixels are considered as initial population for the genetic algorithm. The intensity values of the border points are then converted as 8 bit binary strings, and these values are considered as population strings and intensity values are considered as fitness value for genetic algorithm. Now the genetic operators such as reproduction, single point crossover, and mutation are applied to get new population of strings. Finally, the border pixel, which generates the minimum value of the fitness, is considered as the nipple position. Fig. 8 shows the single point crossover operation. Fig. 9 shows the single point mutation operation. Fig. 10

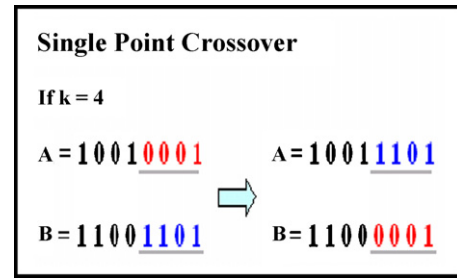
Fig. 8 – Single point crossover operation.

Fig. 9 – Single point mutation operation.

Step 1 : S_{ij}← Original Image;
$\quad\quad\quad$ B_{ij} ←Border image;
Step 2 : [m n] $\quad$ ← size of B_{ij}
Step 3 : **for** each border pixel in B_{ij}
$\quad\quad\quad$ G← intensity of the border pixel from S, converted to binary string
$\quad\quad\quad$ F← fitness value; intensity values of the pixels
$\quad\quad\quad$ Pop1← initial population contains G
$\quad\quad\quad$ **end**
$\quad\quad\quad$ p ← 1
Step 4 : **repeat** for N times
$\quad\quad\quad$ **for** each string in Pop1
$\quad$ g1, g2 ← select two strings for reproduction. For the selection of two strings roulette wheel is implemented as follows:
(i) $\quad$ r = random() * sum_of_fitness
$\quad\quad$ [Hint: random() function returns a random number between 0 and 1]
(ii) $\quad$ psum = 0, i=0, m → size of the population
(iii) $\quad$ p → contains the population strings
(iv) $\quad$ psum = psum + p(i)
(v) $\quad$ i = i + 1
(vi) $\quad$ if ((i <= m) and (psum < r)) Goto Step: (iv)
$\quad\quad$ return i
(vii) g3, g4← new strings after cross over.
A: $\;$ g5, g6 ← strings after mutation
B: Pop2(p) ← g5;
$\quad\quad$ p ← p+1; Pop2(p) ← g6;
$\quad$ **end**
$\quad$ min ← Min(Pop2); Pop1 ← Pop2;
$\quad$ pos ← where the B(i,j) = min;
$\quad$ **end**

Fig. 10 – Algorithm of identification of nipple position using genetic algorithm.

Step 1. S_{ij}← Original Image; B_{ij} $\quad$ ←Border image
Step 2. [m n] $\quad$ ← size of B_{ij}
Step 3. for each border pixel in B_{ij}
$\quad\quad$ K ← kernel of the border pixel of size 3×3 from S
$\quad\quad$ F ← fitness value; (sum of the intensity values of all the pixels in a kernel).
$\quad\quad$ Pop1← initial population contains K and F
$\quad\quad$ End
Step 4. $\quad$ repeat for NI times
$\quad\quad$ for each string in Pop1
$\quad\quad$ k1, k2 $\quad$ ← select two kernels for reproduction. For the selection of two kernels roulette wheel is implemented as follows:
i. $\;$ r = random() * sum_of_fitness .
ii. $\;$ partsum = 0, i=0, m → size of the population
iii. $\;$ p → contains the population strings
iv. $\;$ partsum = partsum + p(i)
v. $\;$ i = i + 1
vi. $\;$ if ((i <= m) and(partsum < r)) Goto Step:(iv) else return i
vii. $\;$ k3, k4← new kernels after crossover. The newly reproduced kernels are crossed over by exchanging the values in the window with the size of 2×2.
a. $\;$ k5, k6 ← kernels after mutation, here a random bit in the kernel is flipped or flopped. In mutation, if a border configuration that matches one of the 14 configurations in the corresponding and transformation is performed.
b. $\;$ pop2(p) (k5); p (p+1); Pop2(p) (k6);
$\quad\quad$ end
$\quad\quad$ pop1 (pop2);
$\quad\quad$ End

Fig. 7 – Algorithm of detection of breast border using GA.

shows the algorithm of identification of nipple position using genetic algorithm. Fig. 11 shows the output for nipple position using genetic algorithm. Fig. 12 shows the alignment of mammograms.
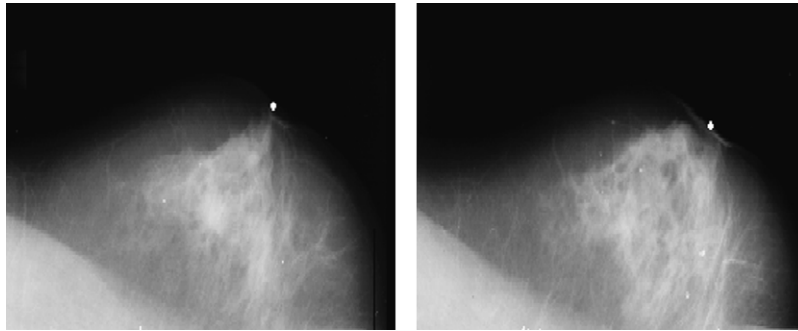
Fig. 11 – Nipple identification using GA.

3.4. Alignment and subtraction

The spatial coordinates of the border points and nipple position are used to determine the angle of rotation to align the mammogram. After the right breast border is displaced, the correlation coefficient between the coordinates of the points of the left breast border and the coordinates of the points of the rotated right breast border are calculated for angles ranging between −5° and +5° with 1° step. The angle corresponding to the maximum value of the correlation coefficient is the angle of rotation of the right breast image, that is, the degrees that need to be rotated for the right breast border to match the left breast border.

3.5. Asymmetry image

After the images are aligned, subtracting the digital matrix of the left and right breast image the disparity is arrived at by means of bilateral subtraction. Microcalcification in the right breast image have positive pixel values in the image obtained after subtraction, while microcalcifications in the left breast image has negative pixel values in the subtracted image.
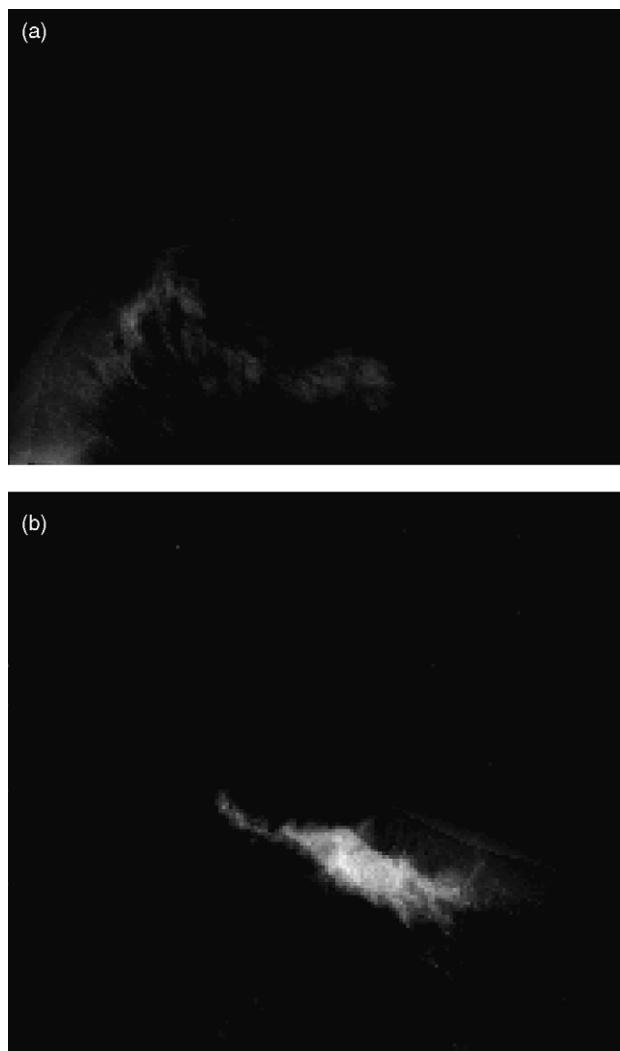
As a result, two new images are generated: one with positive values and the other with negative values. The most common gray value is zero, which indicates no difference between the left and the right images. Simple linear stretching of the two generated images to cover the entire available range of 1024 gray levels was then calculated. The asymmetry image can be thresholded to extract suspicious regions. To generate the ROC curve, the asymmetry image is thresholded using ten different intensity values ranging from 60 to 150. Fig. 13 shows the (a) negative difference image and (b) positive difference image.

4. Experiments and results

The effectiveness of the proposed technique is determined by extracting the suspicious region from the mammogram image using bilateral subtraction. The true positive detection rate and the number of false positive detection rate at various thresholds of the asymmetry images are used to measure the algorithm's performance. These rates are rep-
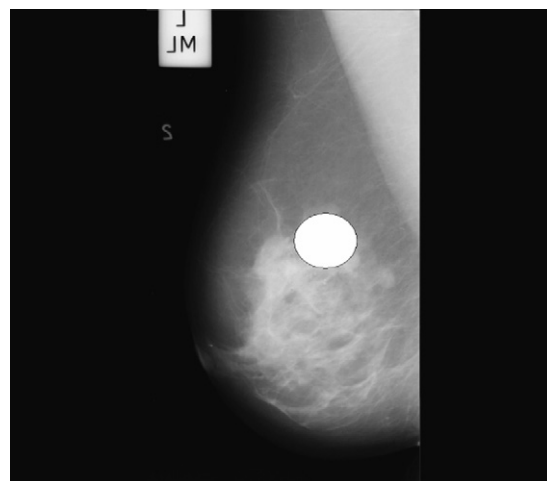

Left image   Right image
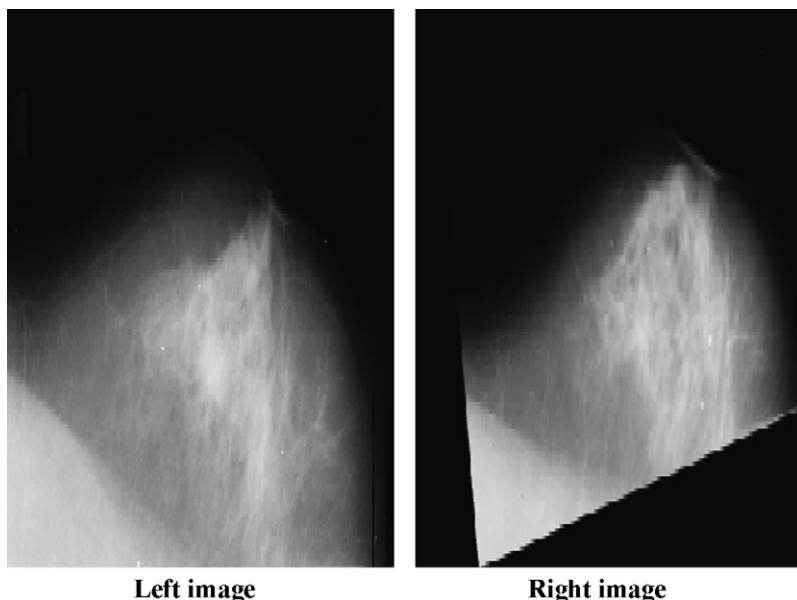
Fig. 12 – Alignment of mammograms.

(a)

(b)

Fig. 13 – (a) Negative difference image and (b) positive difference image.

Fig. 14 – Ground truth image from MIAS database (mdb265.pgm).

Table 1 – TPF and FPF computation				
Threshold	TP	FP	TPF	FPF
50	81	33	0.71	0.2890
60	84	30	0.736	0.2630
70	88	26	0.771	0.2280
80	93	21	0.815	0.1840
90	99	15	0.868	0.1310
100	101	13	0.885	0.1140
110	103	11	0.903	0.0964
120	104	10	0.912	0.0877
130	106	8	0.929	0.0700
140	107	7	0.938	0.0614
150	107	7	0.938	0.0614

resented using receiver operating characteristic curves (ROC) [9].

True positive (TP) and false positive (FP) rates are calculated at 10 different thresholds selected on the segmented image to generate the ROC curve. A region extracted in the asymmetry image that overlaps with a true abnormality as provided on the ground of truth image is called a true positive detection. Fig. 14 shows a ground truth image from the MIAS database. The white region indicates the suspicious region. An overlap means that at least 60% of the region extracted lies within the circle indicating the true abnormality as determined by the MIAS database.

For example, in the mammogram mdb265.pgm, the spatial coordinate position of the suspicious region, x and y are 593, 498, respectively, and the radius is 60 pixels. The resultant asymmetry image obtained from bilateral subtraction contains the suspicious region at (593, 498), with a radius of 60 pixels of the resultant image. Compared to the MIAS information on mdb265.pgm, results from the proposed method overlaps 87% of the specified region, respectively, from each

segmentation and this image is classified as true positive image. Suppose the overlap is less than 60% of the specified region then the image is considered a false positive image.

Previous methods such as [3,14] have taken an overlap region of only 40% as true positive. However, in the proposed method, the true positive is considered only at 60% of overlap. All other regions extracted by the algorithm are labeled false positives. Figure shows the ROC curves generated on the full test set, using 10 operating points from bilateral subtraction. If the threshold value is low true detections may become merged with false positive regions.

4.1. ROC analysis

ROC analysis is based on statistical decision theory, developed in the context of electronic signal detection, and has been applied extensively to diagnostic systems in clinical medicine. The ROC curve is a plot of the classifier's true positive detection rate versus its false positive rate. The false positive (FP) rate is the probability of incorrectly classifying a non-target object (e.g. normal tissue region) as a target object (e.g. suspicious tumor region). Similarly, the true positive (TP) detection rate is the probability of correctly classifying a target object as being a target object.

4.1.1. *Sensitivity versus specificity*

The performance of proposed method is best described in terms of their sensitivity and specificity, quantifying their performance related to false positive and false negative instances. These metrics are based on the consideration that a test point always falls into one of the following four categories:

- False positive (FP) if the system labels a negative point as positive.
- False negative (FN) if the system labels a positive point as negative.
- True positive (TP) and true negative (TN) if the system correctly predicts the label.

The sensitivity or true positive fraction (TPF) is defined as the ratio between the number of true positive predictions and the number of images in the test mammogram set. It is defined as follows:

$$\frac{TPF}{\text{sensitivity}} = \frac{T_P}{(T_P + F_p)}$$

while the specificity or false positive fraction (FPF) is defined as the ratio between the number of false positive predictions and the number of images in the test mammogram set. It is defined as follows:

$$\frac{FPF}{\text{specificity}} = \frac{F_P}{T_P + F_p}$$

The overall accuracy is the ratio between the total number of correctly classified mammograms and the test set size (total number of mages). It is defined as follows:

$$\text{overall accuracy} = \left(\frac{N_r}{N}\right) \times 100\%$$

where N_r is the number of correctly classified mammogram images during the test run and N is the complete number of test mammograms. To make the ROC graph, the X-axis is 1 minus the specificity and the Y-axis is the sensitivity. Draw a diagonal line on the graph from (0, 0) in the lower left hand corner to (1, 1) in the upper right hand corner. The ROC is the best suited to analyze the performances of segmentation and classification. Fig. 14 shows performance of proposed method analyzed by ROC curve. Table 1 shows TPF and FPF computation. Table 2 shows the comparison of detection rate between the previous works and the proposed method. Fig. 15 shows performance analysis.

The area under the ROC curve (Az value) is an important criterion for evaluating diagnostic performance. The ROC curve is in the range between zero and one. The value of Az is 1.0 when the diagnostic detection has perfect performance, which means that TP rate is 100% and FP rate is 0%. The Az value is
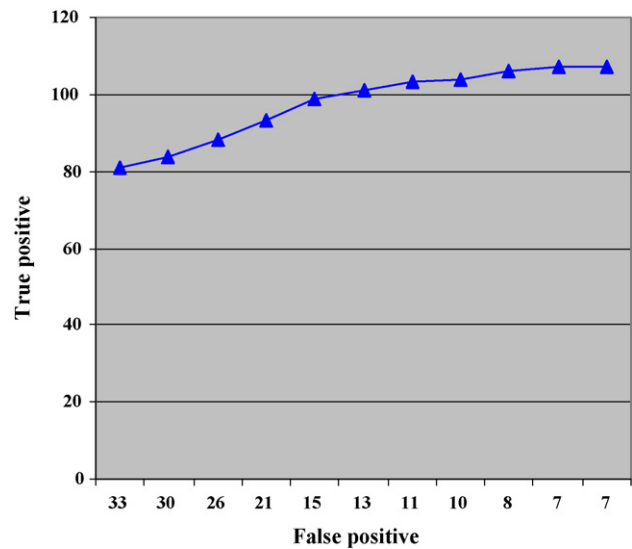

Fig. 15 – **Performance analysis.**

computed by trapezoidal rule. The Az value for the proposed algorithm is 0.906.

5. Summary and conclusion

The bilateral subtractions for mammogram image segmentation have been implemented. The bilateral subtraction method has been designed to detect automatically both the breast border points and nipple position in digital mammograms using GA. In border detection, the border pixel intensity values were considered as population strings. Reproduction was applied to those strings to generate parent strings using fitness values for crossover operator. Crossover and mutation operators were used to generate mated strings, the new population for the detection of border. The detected border is evaluated using figure of merit, which shows that the genetic algorithm detected the border more exactly than other edge detectors. From the extracted border, the border pixels are considered as population strings to GA to find the nipple position.

Having the border points and the nipple position as references, the right mammogram was aligned corresponding to the left mammogram and the left image was subtracted from right image to obtain the asymmetry image. Then the asymmetry image is thresholded to isolate the asymmetries or microcalcifications extracted from the background tissue. To evaluate the performance of the segmentation algorithms the ROC curve was generated. The experimental results show

Table 2 – Performance analyses		
Sl. no.	Authors and methods	Detection rate (%)
1	Ferrari and Rangayyan [6], directional filtering with Gabor wavelets	74.40
2	Lau and Bischof [10], asymmetry measures	85.00
3	Sallam and Bowyer [14], unwarping technique	86.60
4	The proposed metaheuristic approach-GA, bilateral subtraction	90.60

that the bilateral approach produces 0.906 as Az value. It was observed that the metaheuristic GA performed well.

REFERENCES

[1] U. Bick, M.L. Giger, R.A. Schmidt, R.M. Nishikawa, D.E. Wolverton, K. Doi, Automated segmentation of digitized mammograms, Acad. Radiol. 2 (1995) 1–9.

[2] R. Chandrasekhar, Y. Attikiouzel, Automatic breast border segmentation by background modeling and subtraction, in: M.J. Yaffe (Ed.), Proceedings of the 5th International Workshop on Digital Mammography, Medical Physics Publishing, Toronto, Canada, 2000, pp. 560–565.

[3] L.P. Clarke, M. Kallergi, W. Qian, H.D. Li, R.A. Clark, M.L. Silbiger, Tree-structured non-linear filter and wavelet transform for microcalcification segmentation in digital mammography, Cancer Lett. 7 (1994) 173–181.

[4] S. Detounis, Computer aided detection and second reading utility and implementation in a high volume breast clinic, Appl. Radiol. 3 (9) (2004) 8–15.

[5] R.J. Ferrari, R.M. Rangayyan, J.E.L. Desautels, R.A. Borges, A.F. Frere, Analysis of asymmetry in mammograms via directional filtering with Gabor wavelets, IEEE Trans. Med. Imag. 20 (9) (2001) 953–964.

[6] R.J. Ferrari, R.M. Rangayyan, J.E.L. Desautels, R.A. Borges, A.F. Frere, Automatic Identification of the Pectoral Muscle in Mammograms, IEEE Trans. Med. Imag. 23 (2) (2004) 232–245.

[7] D.E. Goldberg, Genetic algorithms in search, in: Optimization and Learning, NY, Addison Wesley, 2000.

[8] M. Gudmundsson, E.A. El-Kwae, M.R. Kabuka, Edge detection in medical images using a genetic algorithm, IEEE Trans. Med. Imag. 17 (3) (1998) 469–474.

[9] H. Jean, M.C. David, F.B. Charles, P. Zygmunt, J.D. Edward, Preclinical ROC studies of digital stereo mammography, IEEE Trans. Med. Imag. 14 (2) (1995) 318–327.

[10] T.K. Lau, W.F. Bischof, Automated detection of breast tumors using the asymmetry approach, Comput. Biomed. Res. 24 (1991) 273–295.

[11] A.J. Mendez, P.G. Tahocesb, M.J. Lado, M. Souto, J.L. Correa, J.J. Vidal, Automatic detection of breast border and nipple in digital mammograms, Comput. Meth. Prog. Biomed. 49 (1996) 253–262.

[12] Z. Michalewicz, Genetic Algorithms, Data Structures, Evolution Programs, Springer-Verlag, Heidelberg, 1996.

[13] W.K. Pratt, Digital Image Processing, 3rd ed., Wiley–Inter science Publication, 2001.

[14] M.Y. Sallam, K.W. Bowyer, Registration and difference analysis of corresponding mammogram images, Med. Image Anal. 3 (2) (1999) 103–118.

[15] M.K.J. Siddiqui, M. Anand, P.K. Mehrotr, R. Sarangi, N. Mathur, Biomonitoring of organochlorines in women with benign and malignant breast disease, Environ. Res. 1 (2004) 1–8.

[16] K. Thangavel, M. Karnan, R. Siva Kumar, A. Kaja Mohideen, Automatic detection of microcalcification in mammograms—a review, Int. J. Graph. Vision Image Process. 5 (5) (2005) 31–61.

[17] K. Thangavel, M. Karnan, CAD system for preprocessing and enhancement of digital mammograms, Int. J. Graph. Vision Image Process. 9 (9) (2006) 69–74.

[18] M.A. Wirth, A. Stapinski, Segmentation of the breast region in mammograms using active contours, Department of Computing and Information Science, University of Guelph, USA, 1998.